International Conference on Space Optics—ICSO 2014

La Caleta, Tenerife, Canary Islands

7–10 October 2014

Edited by Zoran Sodnik, Bruno Cugny, and Nikos Karafolas

Overview of IASI-NG the new generation of infrared atmospheric sounder

F. Bernard

B. Calvel

F. Pasternak

R. Davancens

et al.

International Conference on Space Optics — ICSO 2014, edited by Zoran Sodnik, Nikos Karafolas, Bruno Cugny, Proc. of SPIE Vol. 10563, 105633H · © 2014 ESA and CNES
CCC code: 0277-786X/17/$18 · doi: 10.1117/12.2304101

Overview of IASI-NG the new generation of infrared atmospheric sounder

F. Bernard[1], B. Calvel[2], F. Pasternak[2], R. Davancens[2], C. Buil[1], E. Baldit[1], C. Luitot[1], A. Penquer[1]
[1] Centre National d'Etudes Spatiales (CNES), France. [2]Aibus Defense and Space, France

***Abstract*— The Infrared Atmospheric Sounding Interferometer New Generation (IASI-NG) is a key payload element of the second generation of European meteorological polar-orbit satellites (METOP-SG) dedicated to operational meteorology, oceanography, atmospheric chemistry, and climate monitoring. IASI-NG is designed with a very high level of accuracy being dedicated to operational meteorology, climate monitoring, characterization of atmospheric composition related to climate, atmospheric chemistry and environment. The performance objective is mainly a spectral resolution and a radiometric error divided by two compared with the IASI first generation ones.**
The measurement technique is based on wide field passive Fourier Transform Spectrometer (operating in the 3.5 - 15.5 µm spectral range) based on an innovative Mertz compensated interferometer to manage the so-called self-apodization effect and the associated spectral resolution degradation.
We will present an overview of the instrument architecture and ongoing instrument development.

Keywords: Fourier Transform Spectrometer, infrared, atmosphere, sounding.

I. INTRODUCTION

What about the weather tomorrow? Will Eyjafjallajökull volcano's eruptions allow planes to fly in the coming days? Does our planet become warmer? The challenges of meteorology, atmospheric chemistry and climate monitoring are more and more present in our society and in our daily lives.
For over 25 years CNES invest on spacecraft missions for studying, monitoring and understanding our Atmosphere [1], and especially on spectrometer or interferometer based instruments [2,3,4] for delivering data to operational meteorology community and atmospheric chemistry community.
Thus was born the IASI mission which has been designed for operational meteorological soundings and for atmospheric chemistry by estimating and monitoring trace gases like ozone, methane or carbon monoxide on a global scale. It provides since October 2006 operational data [5] with a very high level of accuracy. The role of the IASI instrument is to monitor the Atmosphere in the infrared band (from 3.6 µm to 15.5 µm) thanks to the use of a Michelson interferometer. For co registration with AVHRR imager present on the same satellite (METOP), IASI has an integrated infrared imager.
The IASI-NG mission [6] aims to provide continuity of the IASI service but with a challenging performances improvement with respect to IASI's ones. The Table 1 gives the main instrument requirements. These new needs exhibit a spectral resolution and a signal-to-noise ratio improved by a factor two compared with IASI. First idea to fulfill the requirements is, compared to IASI, to increase the interferometer Optical Path Difference (OPD) range (to obtain the desired spectral resolution and spectral sampling) and to increase the pupil size and/or the time observing the signal to cope with the radiometric noise.
Increasing pupil size is rapidly difficult due to mass and volume needs for the instrument. Increasing the time of observation is possible by increasing the instantaneous field of view (FOV) of the instrument because we also want to have the same on ground spatial sampling as IASI.
However, it is well known that increasing OPD range and increasing FOV in a classical Michelson interferometer lead to increase the so called self-apodisation function of the instrument which will lead unavoidably in reducing the spectral resolution. Classical Michelson interferometer requires a compromise between FOV, spectral resolution and signal to noise ratio.

Table 1. IASI-NG main requirements

Characteristic	Requirement	Value
Geometry	sounding point size	IASI like (≈12km)
	spatial sampling	IASI like (≈25km)
	geolocation error	IASI/2 (0,5 km)
Radiometry	radiometric calibration error	IASI/2
	NedT@280K	IASI/2
	radiometric error	IASI/2 (≈0,25K @ 280K)
Spectral	continuous spectral covering	IASI like
	spectral resolution	IASI/2
	spectral sampling	IASI/2
	spectral calibration error	IASI/2

The only way to succeed in fulfilling the requirement is to compensate the self-apodisation function due to the FOV. The IASI-NG instrument is based on a classical Michelson interferometer with a Mertz compensator, where a variable plate thickness is introduced in a pupil plane allowing to compensate for each OPD value the optical path difference between the on axis and the off axis rays which is a condition to master the field self-apodisation function. This technique allows having a widened field interferometer. One of the originality of the instrument is in the implementation of the OPD and compensation mechanisms with a unique actuator (single motorization).This will be described in Section III.
The compensation of the field allows to choose a field of 100x100 km² and to implement four by four detectors in the detection chain. This will be described in more detail in Section IV.

II. INSTRUMENT DESCRIPTION

The overall layout on the instrument is given by Fig. 1. The instrument is composed of various sub-systems, the following presents a summary of the instrument functions and operations.
The beam coming from the observed point on Earth enters the instrument via a reflection on a pointing mirror. A two-axis scan mechanism provides the desired target direction and compensates for satellite velocity during the interferogram acquisition. The needed swath (around 2000 km) is covered during a regular cycle which is repeated along the orbit.
In addition to the nominal Earth target acquisition, the scan mechanism allows five dedicated pointing directions to the three instrument calibrations systems:
- one internal black-body and two deep space views for radiometric calibration,
- a Fabry-Perot filter for spectral calibration. The spectral calibration is periodically performed by looking at the cold space through this filter which provides a reference spectrum comb which is used to check the calibration law of the instrument,
- an interferometer wavefront calibration, named Wave Front monitoring System (WFS). It uses a source beam, provided by a laser source, sent from the edge of the field mask located in the entrance telescope towards the pointing mirror.

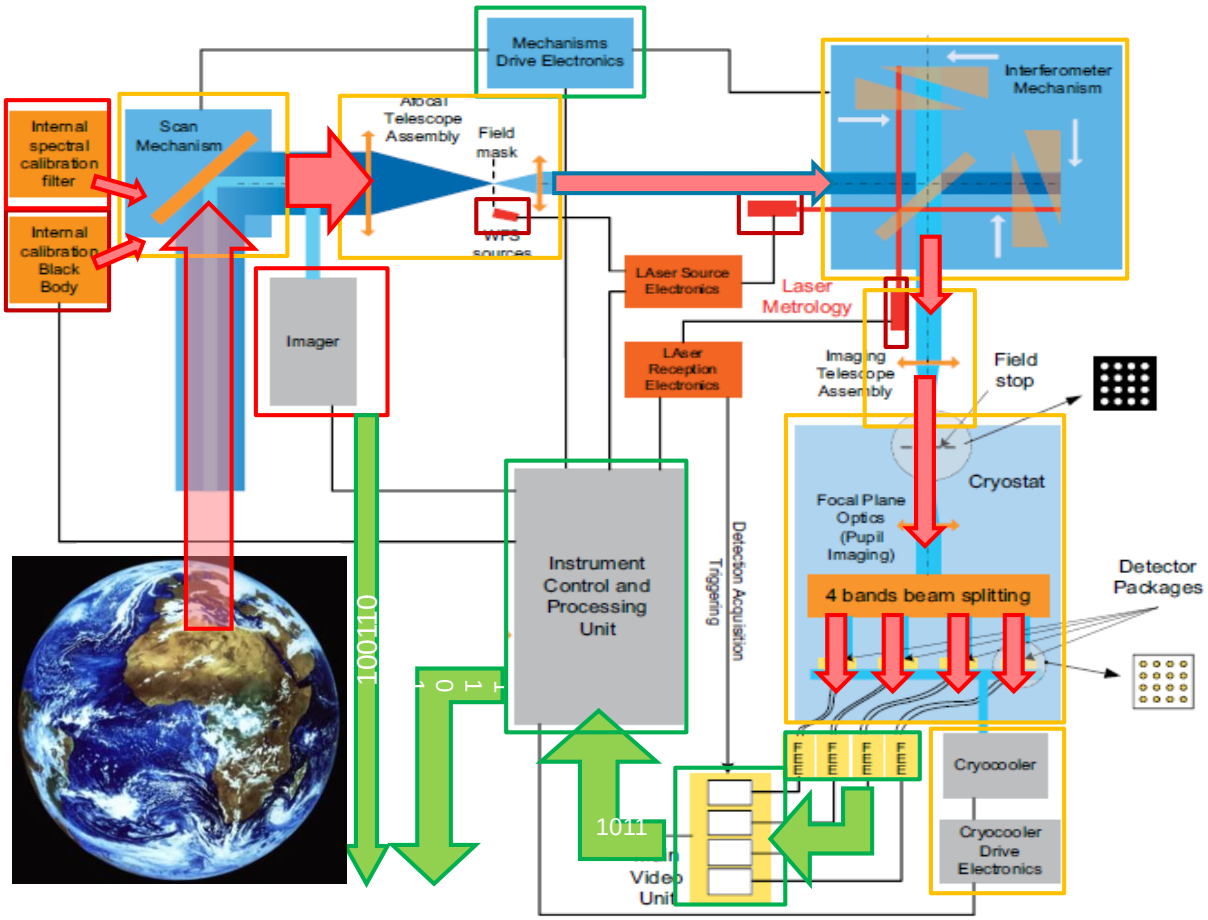

Fig. 1. IASI-NG functional scheme

This latter is used in autocollimation mode to send back the WFS beam into the instrument. Processing of the data acquired with the science detectors of one spectral band allows measuring the interferometer wavefront. These wavefront data are taken into account for ground processing. This operation is foreseen to be performed during commissioning phase and a few times during the mission to check the long-term stability of the interferometer.

A typical observation sequence consists in pointing the scan mirror successively towards the 14 Earth views to cover the required swath (Fig. 2). It is then switched towards two successive radiometric calibration positions, one aiming at a reference Blackbody and one aiming at the cold space. This cycle is then repeated automatically and the instrument performs continuous data acquisition throughout the mission lifetime.

The 90 mm diameter beam then enters the Afocal Telescope Assembly which reimages the entrance pupil inside the interferometer, providing a beam diameter reduction ratio of 2.25: the pupil size is reduced to 40 mm at interferometer level. The resulting field increase is acceptable thanks to the Mertz compensation which allows wide field angles without compromising spectral resolution.

The optical path difference resulting of the interferometer mechanism motion is monitored by the Laser Metrology. A frequency stabilised laser source sends several beams into the interferometer: these beams undergo interferences in the interferometer in the same way as the science beams and specific detectors receive the resulting metrology interference signals. The Laser Reception Electronics acquires and processes these data. A computed OPD is used to synchronise the science detectors acquisitions so that interferogram data are acquired at constant OPD intervals. The laser signals are also used to derive the tilt of the differential wavefront which is used for on ground correction of the instrument spectral response function.
The beam outgoing the interferometer is then focussed by the Imaging Telescope Assembly onto a field stop located at the cryostat input port: this stop consists in a pattern of four by four holes that define the sounder pixels size and relative positions. The cryostat includes the focal plane cold optics and the detectors. The focal plane optics transmits the signal to arrays of four by four detectors in a pupil imaging mode. These optics also include three spectral beam splitters in order to separate the beam into the four IASI-NG spectral bands. Table 2 give the band separation. Compared to IASI a fourth band is needed to fulfil the radiometric noise requirement between 2200 cm^{-1} and 2760 cm^{-1}.

The cryostat allows cooling down of the detectors at the operating temperature of 75 K thanks to a pair of redunded active cryo-coolers. The signals from the detectors are then read and formatted thanks to an analog Front End Electronic (FEE) before been digitised in the Main Video Unit (MVU) and sent to the Instrument Control and Processing Unit (ICPU).

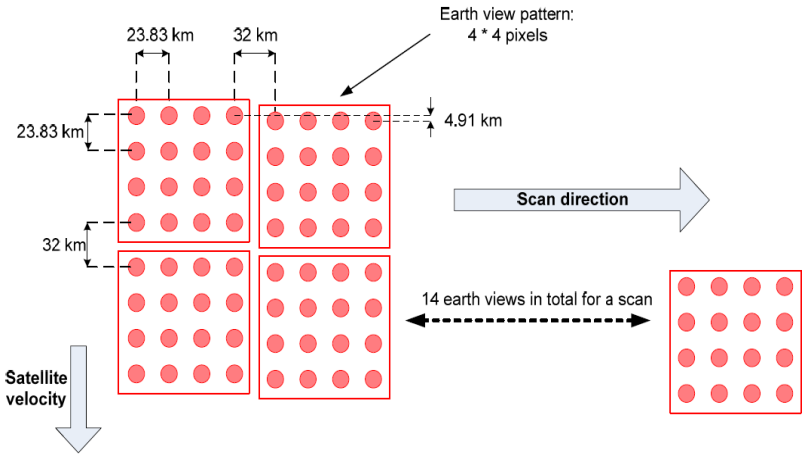

Fig. 2. Instrument FOV footprint on ground and spatial sampling

Table 2. Bands definition

Band	λ	σ
B1	8.70 - 15.5 µm	645 – 1150 cm^{-1}
B2	5.13 - 8.70 µm	1150 – 1950 cm^{-1}
B3	4.35 - 5.13 µm	1950 – 2300 cm^{-1}
B4	3.62 - 4.35 µm	2300 – 2760 cm^{-1}

On board data processing is part of the IPCU. Most of the processing is performed on ground for better flexibility and optimal accuracy. The on board processing is mostly a "compression" processing to cope with the allocated data rate between the instrument and the platform (6Mb/s, raw instrument data rate being ≈120 Mb/s). So, on board processing includes correction of the non linearities and determination of the Zero Path Difference position on the interferograms prior to FFT giving real and imaginary terms of the radiance spectrum. After lossless compression, the spectra are sent on ground together with the metrology tilt data. The sequence of on ground processing performs the self apodisation correction using the metrology tilt data, spectral calibration using Fabry-Perot views and radiometric calibration using the blackbody and cold space interferograms.
The ICPU is also the control electronics of the instrument. It provides the power distribution function, the TM/TC interfaces and the interface with the satellite Spacewire bus. It also performs the instrument FDIR management, the thermal control and the sequencing of the activities.
IASI-NG needs also to geolocate sounding points. This is done thanks to the use of the geolocalisation of METIMAGE images (multiband imager present on METOP-SG [7]) and co-registration with IASI-NG sounding pixels. The co-registation is ensured by a dedicated integrated infrared imager (IMA) inside the IASI-NG instrument. This imager use uncooled microbolometer in the 10,5-12,5 µm band.

III. INTERFEROMETER DESCRIPTION

As already mentioned, the interferometer is a kind of Michelson interferometer modified to introduce a compensation of field self-apodisation. The principle of the compensation technique is to introduce in one arm of the interferometer a thick plate to limit the evolution of the OPD in the field (which is the aspect we would like to supress). Full details on compensation have been reported in [8], Fig. 4 recalls principles.
It is easy to show that there is a relation between the OPD, the mirror displacement D, the plate thickness (e) and the optical index (n) of the plate. On axis this relation is:

$$OPD = 2\left(D + e(n-1)\right) \tag{1}$$

The paraxial condition of the compensation is fulfilled when D, e, n vary simultaneously like:

$$D = \frac{e(n-1)}{n} \tag{2}$$

Everybody could check that for a classical Michelson at OPD=0 the interferometer has no field effect and it is so equivalent for the Mertz to D=0 and so to e=0. The technical challenge is to be able to continuously adapt the plate thickness (e) with the displacement mirror variation (D), that is to say somewhere to synchronize two mechanisms: one for the displacement mirror and another one to adapt the plate thickness to the considered displacement. In the proposed concept the compensation is performed simultaneously with the displacement mirror scan thanks to a dedicated interferometer mechanism principle called the Dual Swing Mechanism (DSM).
This interferometer principle is based on an alternate translation of two pairs of optical prisms in opposite directions (dual swing motion). Each arm contains an internal prism (IP) and an external prism (EP). IP and EP are mounted head to toe and by the way the set IP+EP could be considered as a parallel face blade. A reflective coating will be deposited on the outside face of the EP, so the outside face of EP could be considered as a plane mirror for the interferometer.
OPD is obtained by moving EP (the mirror on the outside face) in one side in an arm and in the other side in the other arm (this also reduces the need of stroke for the mechanism). The movement is in the plane of the hypotenuse of EP. To cope with the compensation condition (2) the IP movement must be such that the images of each outside mirrors are always at the same position at the exit of the interferometer.

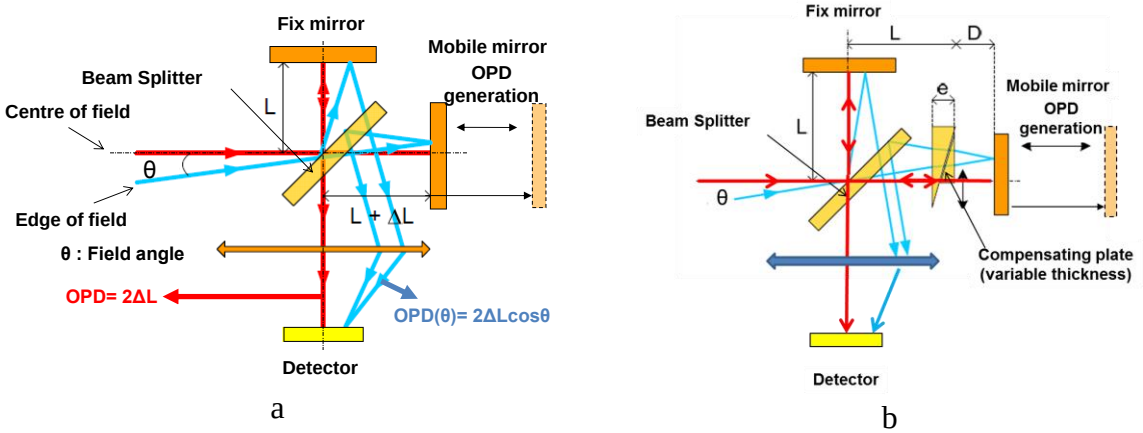

Fig. 4. Michelson Interferometer principle (a) classical (b) with Mertz compensator

So, to do that, in the arm where EP go backward (distance increase between EP mirror and beam splitter) the plate thickness has to increase and in the arm where EP go forward (distance decrease between EP mirror and beam splitter) the plate thickness has to decrease (Fig. 5).

To implement the mechanical displacement, two IPs are mounted on the same supporting frame head to toe (first swing) and the two EPs are mounted on another frame (second swing) head to toe (and of course each IP is mounted head to toe wrt its EP). The adequate movement of translation between the prisms is provided by deformable parallelogram principle. Composed of four articulated levers, the parallelogram provides by its deformation a differential translation between two of its levers, the frames supporting the optical parts as represented on Fig. 6. The resulting frame motions translate the prisms transversally to the optical beam, generating the variation of both mirror and plate thickness. The ratio of thickness variations being obtained by the ratio of the actuation radius of the two frames, and so the accuracy of the compensation, that is to say the synchronization of the mirror displacement and the plate thickness variation, is obtained purely by mechanical considerations. The circular motion of the lateral panels also generates a pure translation (transverse motion) of the prisms which has no effect on the optical performance because the variation is identical on both interferometer arms.

The proposed design is so a plane mirrors interferometer and so the DSM has to ensure a dual swing motion of the prisms with minimum parasitic tilts together with a sufficient high kinematic stability along the stroke.
In order to check the feasibility and the performances of the design, a mock up of the DSM has been studied. This mock-up aims to demonstrate the principle of the compensated interferometer. For ease of implementation this mock-up is designed for the visible domain which is a worst case when considering compensation efficiency (Fig. 7). Procurement and assembly of this mock-up is now finished and validation phase have started. First interferograms of a monochromatic source have been obtained. Some mechanical and thermal validations have also allowed verifying the stability of the concept under environment.

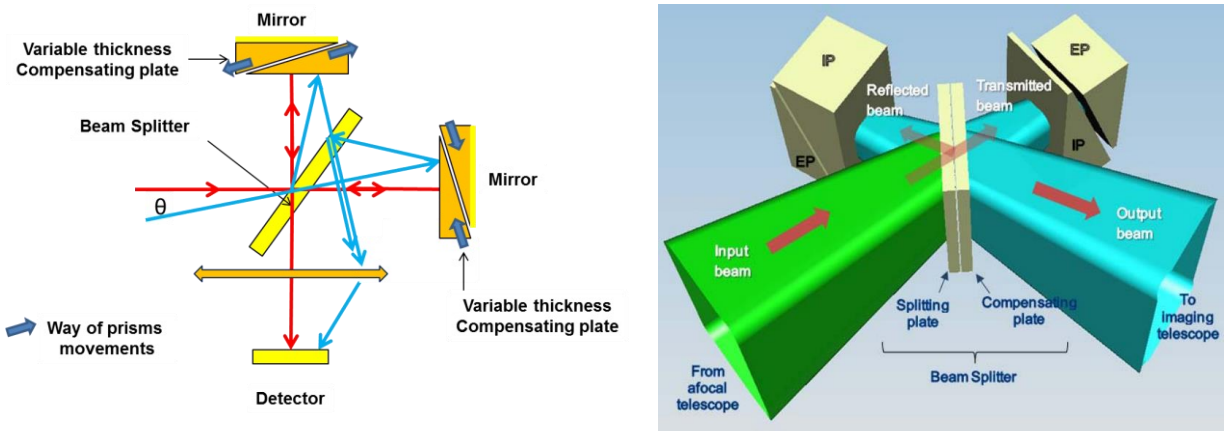

a b

Fig. 5. DSM description (a) principle (b) scheme of implementation

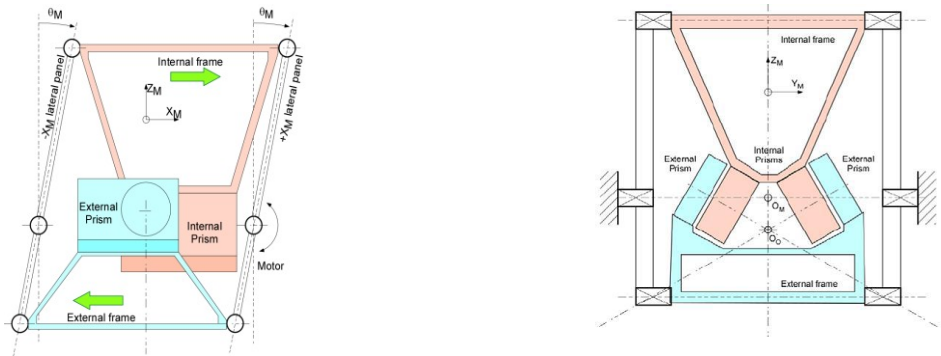

Fig. 6. DSM mechanical description

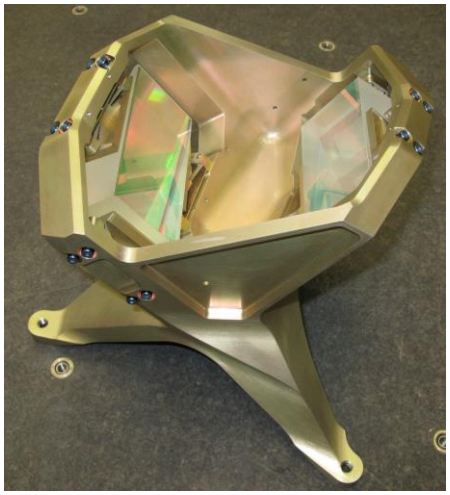

Fig. 7. Mock-Up of Internal Prism Frame in the visible domain

IV. ACQUISITION CHAIN DESCRIPTION

In parallel with the development of the optical chain, the development of the detection chain has also to be conducted to master the overall instrument development plan. IASI-NG detection chain may seem comparable to IASI's one but it is quite different in its operating point and implementation.

A. General organization

As described, the detection chain is composed of Detector Packages (DP), analog Front End Electronics and Main Video Unit. The science domain has been divided into 4 bands and we will have four by four detectors in each band. In order to minimize mission unavailability in case of failure, the detection chain architecture is organized to lost non- adjacent pixels and no more than 25% of the useful pixels in case of failure of an equipment in the chain. That is to say that the chain is divided into 4 groups of 2x2 pixels in each band, each group being independent of the others and composed of non-adjacent pixels as described in Fig. 8.

B. B1 Chain

The B1 band will be made with an array of 4x4 PC MCT detectors [9]. To improve the responsivity each monolith detector will be "multi-striped" (Fig. 9) to increase impedance and thereby reduce the need for very low noise floor of the downstream electronics. Use of this kind of detectors is made possible thanks to the pupil imaging. Use of PC detectors for band B1 also allows getting the right detectivity with reasonable cooling. Several mock-up have already been fabricated and tested and show preliminary performances in line with the needs.

C. B2 to B4 Chain

The B2 to B4 bands will use MOVPE PV detectors made also with MCT material [10]. Detector circuit will be hybridized on analog CMOS circuit containing a Transimpedance Amplifier (TIA) allowing to drastically increase the signal-to-noise ratio at the output of the cryostat. Needs for detection circuit are in line with state of the art performances for detectors in this wavelength. The CMOS readout circuit is under detailed conception with a view to go to foundry in Q3-2014.

Fig. 8. Distribution of the 4x4 soundings pixels in 4 groups (materialized by colours) of 2x2 non-adjacent pixels

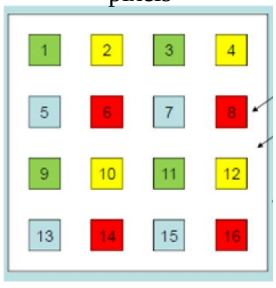

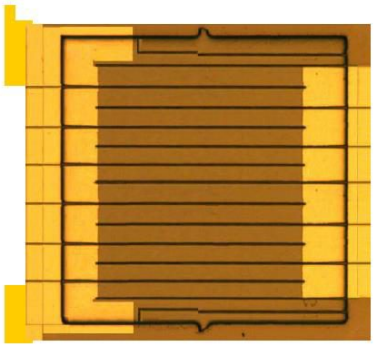

Fig. 9. Mock-up of individual B1 PC Detector Monolith/element (Courtesy of Selex ES)

IV. INSTRUMENT BUDGETS

The IASI-NG instrument will be composed of two modules:
- an Optical Head (called I-OH) that mainly includes opto-mechanical parts of IASI-NG instrument, for the sounder and the imager,
- an Electronics Module (called I-EM) that includes most of the electronics, except for the Front End Electronics, kept close to cryostat, the Imager Video Electronics located in the vicinity of the imager optics and the LASE (Laser Source Electronics) which is located inside the I-OH to avoid having optical fibres between the two modules.

The volume of the two modules is given in Fig. 10. The mass allocation for the overall instrument is 360 kg and the Power budget is about 500W.
The Table 3 recalls the main characteristics of the instrument.

Table 3. Instrument main characteristics

Characteristic	Value / design
Instrument Principle	Bilateral Michelson interferometer with a Mertz compensator
Swath	99.4 °
Instrument Field Of View	4x4 pixels in a box of 100x100 km² Inter-pixel = 23.83 km Inter-scan = 32 km
Sounding Pixel Size	Equivalent to circle of Φ=12 km at nadir
Pupil size	90 mm (40 mm in IFM, reduction ratio 2,25)
Cycle Scan	14 EW + 2 Calibrations + 3 transitions – duration ≈15,6 s
Spectral sampling	Constant OPD sampling
Radiometric Calibration	1 BB et 1 CS on each line
Spectral Calibration	Fabry-Perot and associated Model of the instrument
Optics	input telescope and imagery telescope : Three Mirror Anastigmat optical design
Detectors Package	PC Mono-elements in B1. PV Mono-elements in B2 to B4 - Cryogenic CMOS TIA
Cryocooling	Active redunded Cryocooler. Focal plane at 75 K
On board metrologies	Several lasers : OPD & tilt measurement Wave Front Sensor
Imager	Integrated and based on microbolometers

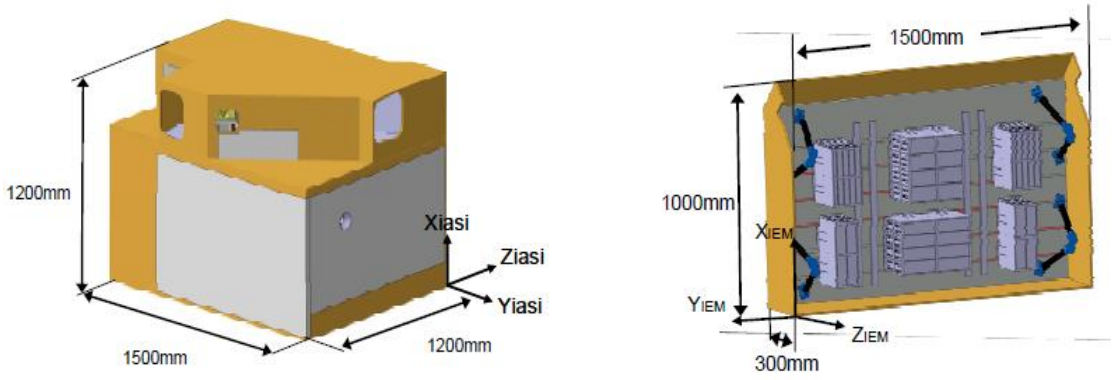

a b

Fig. 10. Instrument volume (a) I-OH – (b) I-EM

V. CONCLUSIONS

Phase B of the IASI-NG Instrument is now running and studies of all sub-system have been started. A global overview of the instrument design has been reported in this paper, however a lot of design trade-off and technological evaluations are actually running to ensure the performance and the quality of the instrument.
The interferometer will be the heart of the instrument. The DSM will allow having a wide field interferometer which is needed to succeed in both radiometric and spectral improvements that IASI-NG have to reach to fulfill the mission requirements. Intensive work is done on study of this sub-system to find the best operating point and the most mature technological solution. This work is completed by mock-up development and measurement which is essential in the development plan. Updated version in the Infrared domain of the DSM is expected before instrument PDR.
Huge work is also under progress on detection chain activities, and especially on detectors packages in order to master the criticality of the detection chain. Derisking this technical domain is also a key element for the success of the instrument.
Finally, processing and calibration approaches are also under definition and evaluation in order to be able to deliver data to user having minimal instrument's signature.
More information can be found on the CNES website http://smsc.cnes.fr/IASI-NG/index.htm

REFERENCES

[1] http://smsc.cnes.fr/html-images/atmosphere.htm
[2] G. Chalon, F. Cayla, D. Diebel, "IASI : An Advanced Sounder for Operational Meteorology" , Proc. Congress of IAF 52, 1-5 Oct. 2001.
[3] C. Pierangelo, P. Hébert, C. Camy-Peyret, C. Clerbaux, P. Coheur, T. Phulpin, L. Lavanant, T. Tremas, P. Henry, A. Rosak, "SIFTI, a Static Infrared Fourier Transform Interferometer dedicated to ozone and CO pollution monitoring," International TOVS Study Conference (ITSC XVI), 5-13 may 2008, Angra dos Reis, Brasil.
[4] C.Buil, V.Pascal, J. Loesel, C. Pierangelo, L. Roucayrol, L. Tauziede, "A new space instrument concept for the measurement of CO2 concentration in the atmosphere," SPIE 8176-12 Remote Sensing Europe, Prague, 2011.
[5] L. Buffet, E. Pequignot, D. Blumstein and al, "IASI instrument onboard Metop-A : Lessons learned after almost two years in orbit", Proc. ICSO Conference, Oct. 2008.
[6] C. Crevoisier, C. Clerbaux, V. Guidard, T. Phulpin et al, "The IASI-NG mission: Scientific objectives and expected results," 3rd IASI Conference Hyères, 4-8 February 2013.
[7] F. Schmülling, I. Zerfowski, A. Pillukat, R. Bonsignori, "METimage : a multispectral imaging radiometer for the EUMETSAT Polar System follow-on satellite mission", Proc. SPIE 7826, Sensors, Systems, and Next-Generation Satellites XIV, 78260P (October 13, 2010)
[8] C. Luitot, J. Boyadjian, C. Buil, F. Pasternak, "Optical Architecture of the new generation Infrared Atmospheric Sounder Interferometer (IASI-NG)," SPIE 8841-22, Current Developments in Lens Design and Optical Engineering XIV, San Diego, August 2013.
[9] I.M. Baker, M.P. Hastings, L.G. Hipwood, C.L. Jones, P. Knowles, "Infrared detectors for the year 2000", III-Vs Review, Volume 9,Issue 2, April 1996, Pages 50-58,60, ISSN 0961-1290
[10] L. Hipwood, C. Maxey, N. Shorrocks, R. Wilson, "MOVPE-Growth of HgCdTe for Infrared Focal Plane", Arrays. Proc OPTRO-12 066 (2012).